



ELSEVIER

Available online at www.sciencedirect.com

SCIENCE @ DIRECT®

Solar Energy Materials
& Solar Cells

Solar Energy Materials & Solar Cells 81 (2004) 339–348

www.elsevier.com/locate/solmat

Structure and optical properties of M/ZnO (M = Au, Cu, Pt) nanocomposites

U. Pal^{a,b,*}, J. García-Serrano^a, G. Casarrubias-Segura^a,
N. Koshizaki^c, T. Sasaki^c, S. Terahuchi^c

^a *Instituto de Física, Universidad Autónoma de Puebla, Apdo. Postal J-48, Puebla 72570, Mexico*

^b *Instituto Mexicano del Petroleo, Eje Central Lazaro Cardenas 152, CP 07730, DF, Mexico*

^c *National Institute of Advanced Industrial Science and Technology (AIST), Nanoarchitectonics
Research Center, Central 5, 1-1-1 Higashi, Tsukuba, Ibaraki 305-8565, Japan*

Abstract

Metal (Au, Cu, Pt)/zinc oxide nanocomposite films were prepared with different metal contents by radio frequency co-sputtering technique. The films were annealed at different temperatures in an argon atmosphere for 2 h. Formation of metal nanoparticles was studied by transmission electron microscopy (TEM) and X-ray diffraction (XRD). UV-Vis optical absorption spectroscopy was used for optical characterization of the samples. With the increase of annealing temperature, the size of the metal particles in the ZnO matrix varied. Surface plasmon resonance bands were observed in the Au/ZnO and Cu/ZnO composite films due to the formation of nanometer-size Au and Cu particles in the matrix. However, a similar behavior was not seen with Pt/ZnO composites. Upon incorporation of Pt nanoparticles in the ZnO matrix, the optical band gap of the matrix was drastically reduced.

© 2003 Elsevier B.V. All rights reserved.

Keywords: M/ZnO; Nanocomposites; Structural properties; Optical properties

1. Introduction

Nanocomposite films that consist of small metal particles in the range of a few to several nanometers (nm) embedded in metal oxides have attracted attention due to their many useful electronic and optical properties as a result of quantum size effects [1,2]. These systems find useful applications in catalysis, photocatalysis, sensors and novel optoelectronic devices. Several techniques like ion implantation [3], sputtering [4], and electrodeposition [5] have been used to prepare nanocomposite films with

*Corresponding author. Tel.: +52-22-2295500; fax: +52-22-2295611.

E-mail address: upal@sirio.ifuap.buap.mx (U. Pal).

silica or glass matrix. However, the use of functional matrix materials like ZnO, MgO and Al₂O₃ for the preparation of nanocomposites is relatively recent [6,7]. Recently, ordering of metal atoms in semiconductor compounds is attracting more interest because they are not thermodynamically stable under bulk growth condition. Furthermore, it is accompanied by change in the band gap even for fixed composition.

In the present work, we prepared several metal/ZnO nanocomposites like Au/ZnO, Cu/ZnO and Pt/ZnO by radio frequency (r.f.) co-sputtering technique and carried out their structural and optical characterizations. The formation of nanometer size metal particles in ZnO matrix and their evolution on post-deposition thermal annealing and with the variation of metal content in the films have been studied by electron microscopy, X-ray diffraction and optical absorption spectroscopy techniques. The optical band gap of the ZnO matrix was drastically reduced from 3.32 to 2.1 eV on incorporation of Pt nanoparticles in them.

2. Experimental

M/ZnO (M = Au, Cu, Pt) nanocomposite thin films containing different metal contents were deposited on quartz glass substrates by r.f. co-sputtering technique. For the preparation of the Au/ZnO and Pt/ZnO composite films, three pieces of Au and Pt wires of 0.4 mm diameter were placed symmetrically on a 100 mm diameter ZnO target and sputtered with 100 W r.f. power at 4 mTorr Argon gas pressure. The content of Au and Pt in the films varied by changing the length of Au and Pt wires (1, 3 and 7.5 mm for Au and 3, 7.5 and 15 mm for Pt) on the ZnO target, keeping the deposition time fixed (1 h). Cu/ZnO nanocomposite films were prepared by co-sputtering of Cu (0.25 mm diameter and 2 mm length wires) and ZnO target (50 mm diameter) with 200 W power at 20 mTorr Argon gas pressure for 2 h. The content of Cu in the films was varied by changing the number of Cu wires on the ZnO target. The thickness of the as-deposited films was measured by a surface profilometer. The thickness of the composite films varied from 0.4 to 0.75 μm with the variation of metal content in them. Some as-deposited films were annealed at different temperatures for 2 h in argon atmosphere. For TEM study, the films were deposited on carbon-coated NaCl substrates and transferred subsequently to the copper grids. For the microstructural characterization a JEOL-2010 electron microscope was used. Optical absorption spectra of the films were measured at room temperature using a Shimadzu UV-Vis-NIR 3101 PC double beam spectrophotometer over the 200–800 nm wavelength range. XRD patterns were recorded using Cu-Kα radiation of a Bruker diffractometer.

3. Results and discussion

From the TEM micrographs we could observe the formation of homogeneously distributed metal nanoparticles in the ZnO matrix. Fig. 1 shows the TEM

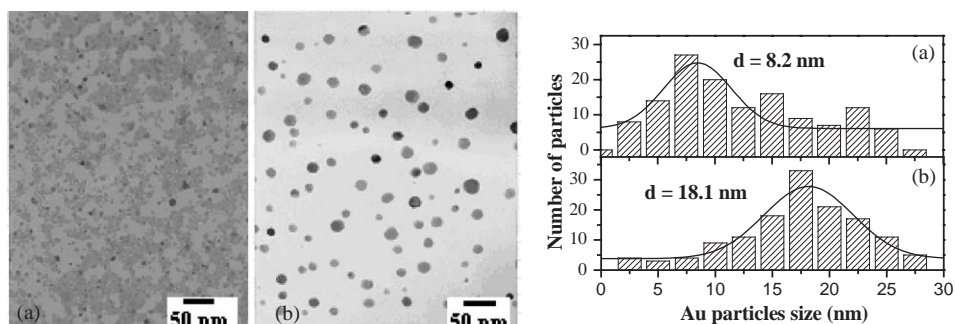


Fig. 1. Typical TEM micrographs of Au/ZnO composite thin films prepared with 3 pieces of Au wires of 7.5 mm length and annealed at: (a) 500°C and (b) 700°C and the size distribution of the Au particles in them.

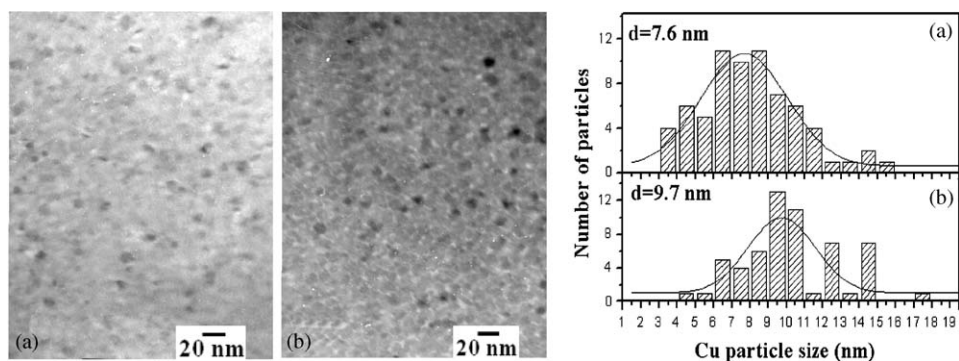


Fig. 2. Typical TEM micrographs of Cu/ZnO composite films annealed at 400°C and prepared with: (a) 4 pieces and (b) 16 pieces of Cu wires of 2 mm length and the size distribution of the Cu particles in the matrix.

micrographs of the Au/ZnO nanocomposite thin films with same Au content but annealed at different temperatures. In general, the average size of the Au particles increased with the increase of annealing temperature. It has been observed that the increase of Au content in the composite films cause only an increase in the density of the particles, without causing any significant change in their average size.

For the Cu/ZnO composite films, we can observe the nanoparticles of size ranging from 2 to 17 nm dispersed in the matrix. With the increase of Cu content in the films, the size and the density of the particles increased. For the films containing higher Cu contents the size of the particles increased with the increase of annealing temperature. However, for the films with lower Cu contents the size of the particles did not increase noticeably on annealing. In Fig. 2, the TEM micrographs of the Cu/ZnO composite films with different Cu content are shown.

Pt nanoparticles were formed in the ZnO matrix on co-sputtering of Pt and ZnO. Fig. 3 shows the typical TEM micrographs of Pt/ZnO composite films prepared with

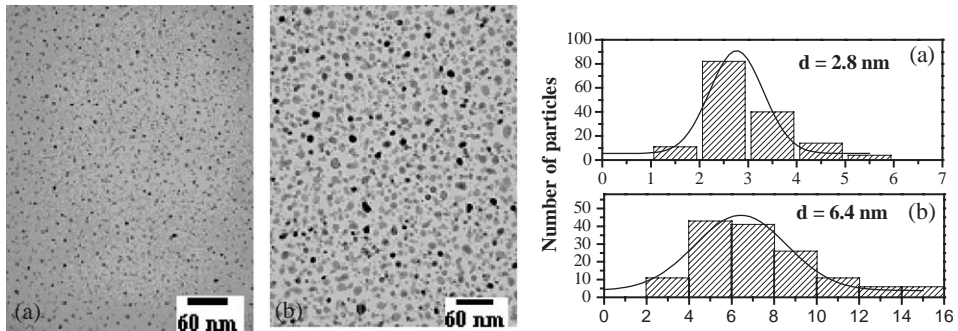


Fig. 3. Typical TEM micrographs of annealed (600°C) Pt/ZnO composite films prepared with 3 pieces of (a) 3 mm and (b) 15 mm length Pt wires and the size distribution of the Pt particles.

different Pt contents and annealed at 600°C. The corresponding size distributions were measured from the micrographs and presented in Fig. 3. In the composite films prepared with 3 pieces of Pt wires of 3 mm length, the size of the Pt particles was in the range of 1–6 nm, with an average size of 2.8 nm. The increment in the Pt content in the films caused a small increase in the average size of Pt particles. For the films prepared with 3 × 15 mm of Pt wires, the average size of the nanoparticles was 6.4 nm. On the other hand, in the as-deposited films prepared with higher Pt content we could observe the agglomeration of small particles to form very big clusters of average size of 275 nm. On thermal annealing at 200°C or higher temperatures the size of the particles decreased drastically due to the disintegration of small Pt particles remained in the bigger clusters. When the annealing temperature increased to 400°C, the dimension of the nanoparticles did not increase noticeably. However, on annealing at 600°C, the small particles aggregated to form particles with an average size of 6.4 nm.

In Fig. 4a, the evolution of the XRD spectrum with the variation of Au content for Au/ZnO composite films annealed at 700°C is shown. With increase of Au content, the intensity of the peaks related to the (111) and (220) planes of Au increase. There appeared a peak corresponding to the formation of Au₂O₃, intensity of which decreased with the increase of Au content in the films. Fig. 4b shows the XRD patterns for the Au/ZnO composite films before and after annealing at different temperatures. With the increase of annealing temperature, the intensity of the (002) and (103) reflections of ZnO increased. However, the intensity of the reflection corresponds to oxidized Au (AuO and Au₂O₃) decrease and the intensity of the (111) reflection corresponds to Au increased. It is clear that on increasing the annealing temperature, the Au in oxidized state is reduced to metallic gold.

Fig. 5 shows the X-ray diffraction patterns for the Cu/ZnO composite films. XRD patterns revealed the peaks related to the (200) plane corresponding to Cu and (110) plane of oxidized Cu along with the peaks corresponding to ZnO matrix. With the increase of annealing temperature, the crystallinity of the ZnO matrix increased gradually and the peak corresponding to Cu₂O became more intense. On increasing the annealing temperature to 300°C or above an increase in the intensity of the peak

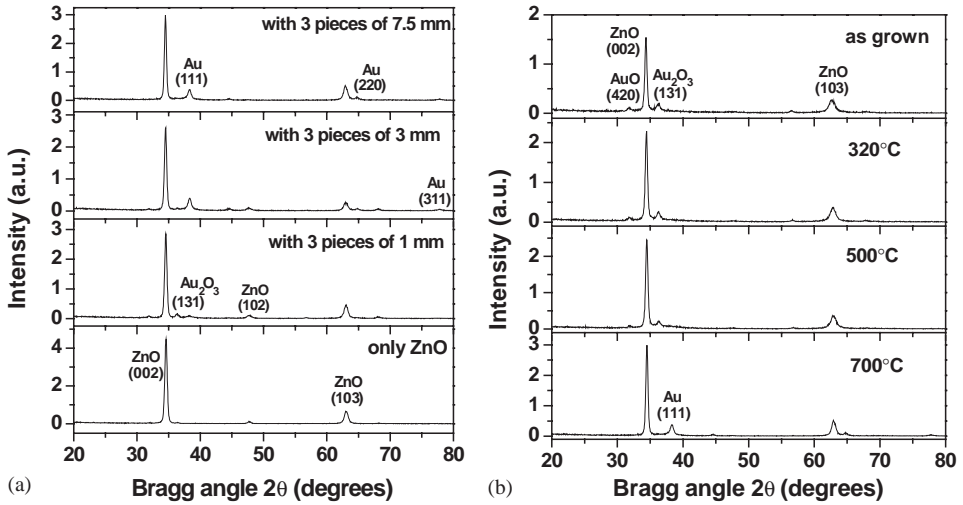


Fig. 4. XRD pattern of the Au/ZnO nanocomposites: (a) prepared with different Au content and treated at 700°C, and (b) prepared with 3 pieces of Au wires of 7.5 mm and annealed at different temperatures.

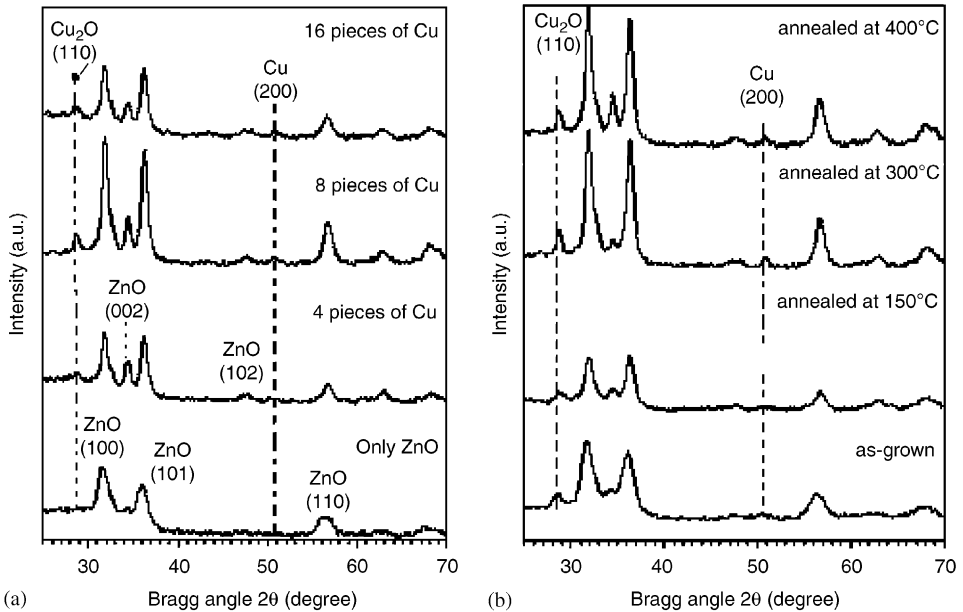


Fig. 5. XRD pattern of the Cu/ZnO nanocomposites: (a) with different Cu content and annealed at 400°C, and (b) prepared with fixed Cu content (16 pieces of Cu wires) and annealed at different temperatures.

corresponding to elemental Cu was observed. With the increase of the Cu content in the films the intensity of the peaks corresponding to elemental and oxidized state of the Cu increased.

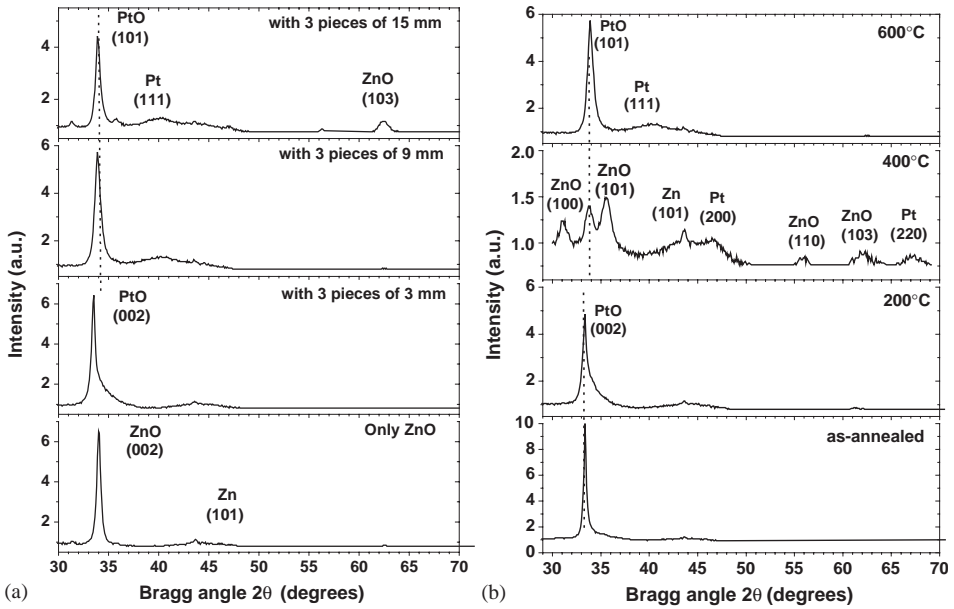


Fig. 6. XRD pattern of the Pt/ZnO nanocomposites: (a) with different Pt content and annealed at 600°C and (b) prepared with 3 pieces of 9 mm Pt wires and annealed at different temperatures.

Fig. 6a shows the X-ray diffraction patterns for Pt/ZnO composite films grown with different Pt contents and annealed at 600°C. The pattern of ZnO revealed two peaks related to the (002) and (101) planes of the crystalline matrix. For the samples grown with 3 pieces of 3 mm Pt wires, a peak was identified as the (002) reflection of PtO. However, a lower intensity of the PtO peak is obtained when the content of Pt increased. This behavior indicates that the effect of oxidation of Pt is lower when the content of Pt is high in the composites. In the spectrum for the samples prepared with pieces of 9 mm length Pt wires, a peak corresponding to the (111) reflection of Pt was identified.

Formation of metal nanoparticles in the composite films is evident from their optical spectra. It is well known that small metallic particles show the optical absorption due to surface plasmon resonance in the ultraviolet-visible region. Fig. 7 shows the optical absorption spectra of the Au/ZnO thin films with different Au content in the matrix (I) and annealed at different temperature (II). There appeared a broad absorption band in the spectral range of 450–800 nm for all the films, the intensity of which increased systematically with the variation of Au content and the temperature of annealing. It is evident that the absorption band is due to the surface plasmon resonance of the Au nanoparticles. With the increase of annealing temperature, the position of the peak shifted gradually towards higher wavelengths. This effect is attributed to the increment in the particle size caused, as mentioned above, by the increases of the annealing temperatures of the samples.

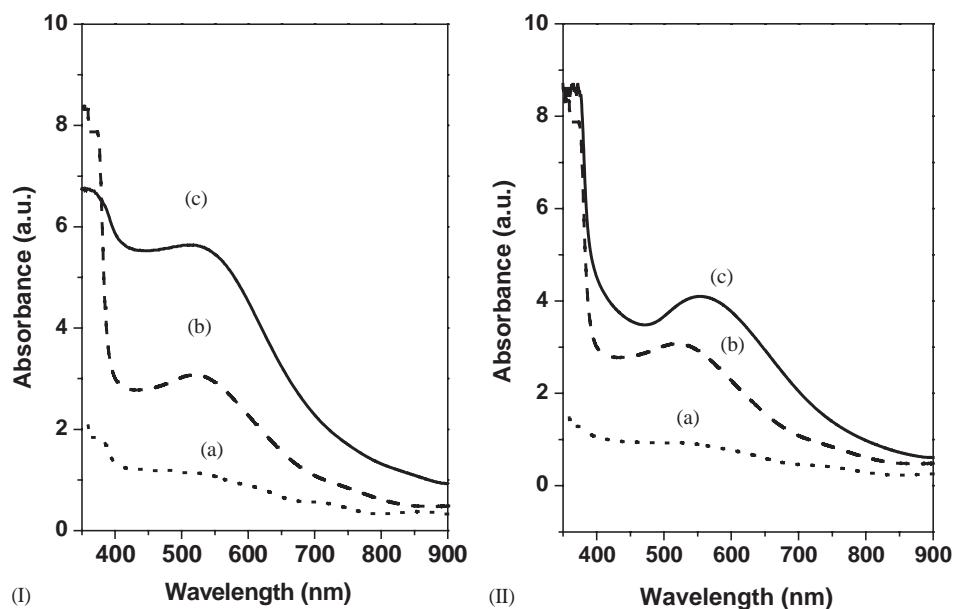


Fig. 7. Optical absorption spectra of Au/ZnO nanocomposite thin films: (I) Prepared with 3 pieces of Au wires of (a) 1 mm, (b) 3 mm and (c) 7.5 mm length and annealed (500°C). (II) Au/ZnO nanocomposite films prepared with 3 pieces of Au wires of 3 mm length; (a) as-grown; (b) annealed at 500°C and (c) annealed at 700°C.

Fig. 8 shows the typical optical absorption spectra for the Cu/ZnO composite films. The spectra revealed an absorption band at around 560 nm, which was assigned to the surface plasmon resonance of Cu nanoparticles. The intensity of the surface plasmon resonance band did not change very much with the increases of the Cu content in the films. However, with the increase of annealing temperature, the intensity of the absorption band increased sharply and its position shifted from 540 to 590 nm. Such behavior is due to the growth of Cu particles caused by the increase of annealing temperature.

The optical band gap for the ZnO in M/ZnO (M = Cu, Pt) composite films was determined by extrapolating the linear portion of $(\alpha h\nu)^2$ versus photon energy ($h\nu$) plots and are shown in Tables 1 and 2. For the undoped ZnO matrix, it may be noted (Table 1) that, as the annealing temperature increased, the band gap energy decreased. The energy gap was 3.32 eV for the as-deposited ZnO films and it decreased to 3.25 eV when the films were annealed at 400°C. This behavior may be attributed to an increase in the crystalline phase of the ZnO matrix. For the Cu/ZnO nanocomposites grown with different Cu content we can observe that the band gap energy corresponding to the as-deposited films increased with the increase of Cu content in them. The increases of energy gap with the increases of Cu content is due to the well known Burstein-Moss shift [8]. On the other hand, for the Pt/ZnO composite films the direct band gap energy of the matrix decreased on increasing the content of Pt in the films. On annealing the composite films, the band gap decreased

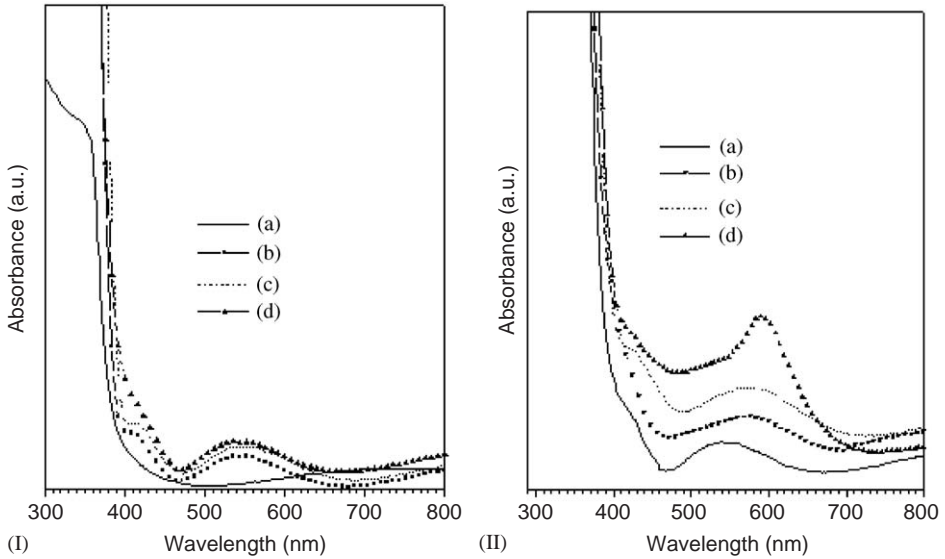


Fig. 8. Optical absorption spectra of Cu/ZnO nanocomposites: (I) As-deposited and prepared with (a) only ZnO; (b) 4 pieces of Cu wires; (c) 8 pieces of Cu wires and (d) 16 pieces of Cu wires. (II) Prepared with 16 pieces of Cu wires and annealed at: (a) as-grown; (b) 150°C; (c) 300°C and (d) 400°C.

Table 1

The band gap values of ZnO matrix for Cu/ZnO nanocomposite films estimated from the absorption spectra

Cu/ZnO composite films	As-deposited	150°C	300°C	400°C
Only ZnO (0 pieces of Cu wires)	3.32	3.27	3.26	3.25
With 4 pieces of Cu wires	3.33			
With 8 pieces of Cu wires	3.34			
With 16 pieces of Cu wires	3.35			

Table 2

The band gap values of ZnO matrix for Pt/ZnO nanocomposite films estimated from the absorption spectra

Pt/ZnO composite films	As-deposited	200°C	400°C	600°C
Only ZnO (0 pieces of Pt wires)	3.32	3.27	3.25	3.25
With 3 pieces of 3 mm length of Pt wires	3.24	3.24	3.24	3.20
With 3 pieces of 9 mm length of Pt wires	3.25	3.23	3.20	2.10
With 3 pieces of 15 mm length of Pt wires	3.1	2.6	2.20	2.10

further. The decrease of band gap of the matrix is basically due to the doping of ZnO by Pt. However, the variation of band gap on the content of Pt incorporation and the annealing temperature is complicated. As the room temperature solubility of Pt in

ZnO is low, incorporation of excess Pt in it did not form a homogeneous dispersion/mixture. This is the reason for the formation of big agglomerates of Pt in as-deposited Pt/ZnO composites prepared with 3×15 mm of Pt wires. On annealing the composite films, those bigger agglomerates dispersed more homogeneously in the matrix due to the increase of solubility of Pt in ZnO and hence formed smaller clusters. On the other hand, due to the increase of solubility of Pt in ZnO, more Pt was incorporated in the matrix even without forming clusters (as dopant) on increasing the temperature of annealing. So, the decrease of band gap energy on increasing the annealing temperature of the composite films is the result of higher Pt doping in ZnO matrix.

4. Conclusions

In conclusion, we report the preparation of M/ZnO (M = Au, Cu, Pt) nanocomposites by r.f. co-sputtering technique. The formation of metal nanoparticles was demonstrated by TEM, XRD and optical absorption spectroscopy. In general, the average size of the metal nanoparticles in the ZnO matrix increases with the increase of metal content in the films. With the increase of the annealing temperature, the average size of the Au and Cu particles in the composites increases. However, in the Pt/ZnO nanocomposites with higher Pt content, we observe the formation of very big clusters of average size of 275 nm. On annealing at 200°C or above the size of the Pt particle decreases drastically, but, when the annealing temperature increases to 600°C the small particles aggregates to form bigger particles. XRD patterns of the M/ZnO composites revealed peaks corresponding to metal in oxidized state which indicates that the metal particles formed in ZnO matrix remain both in its elemental and oxide states. The intensity and position of the surface plasmon resonance absorption band of Au and Cu nanoparticles show a strong dependence on the variation of the metal content and annealing temperature. The optical band gap for the ZnO matrix in the Cu/ZnO composite films shifts towards higher energy with increase of the Cu content, indicating a Brustein-Moss shift due to doping effect. For the Pt/ZnO composite films the direct band gap energy of the matrix decreases on increasing the Pt content in the films.

References

- [1] G. Zhao, H. Kozuka, T. Yoko, *Thin Solid Films* 227 (1996) 147.
- [2] K. Fukumi, A. Chayajara, K. Kadono, T. Sakagushi, Y. Hirono, Gold nanoparticles ion implanted in glass with enhanced nonlinear optical properties, *J. Appl. Phys.* 75 (1994) 3075–3080.
- [3] U. Pal, A. Bautista-Hernandez, L. Ridriguez-Fernandez, J.C. Cheang-Wong, Effect of thermal annealing on the optical properties of high-energy cu-implanted silica glass, *J. Non-Cryst. Solids* 275 (2000) 65–71.
- [4] O. Takai, M. Futsuhara, G. Shimizu, C.P. Lungu, J. Nozue, Nanostructure of ZnO thin films prepared by reactive rf magnetron sputtering, *Thin Solid Films* 318 (1998) 117–119.

- [5] T. Yoshino, S. Takanesawa, T. Ohmori, H. Masuda, Preparation of ZnO/Au nanoparticles thin films by electrodeposition, *Jpn. J. Appl. Phys.* 35 (2) (1996) L1512–L1514.
- [6] N. Koshizaki, K. Yazumoto, S. Terauchi, H. Umehara, T. Sasaki, T. Oyama, *Nanostruct. Mater.* 9 (1997) 587.
- [7] J. García-Serrano, U. Pal, Synthesis and characterization of Au nanoparticles in Al₂O₃ matrix, *Int. J. Hydrogen Energy* 28 (6) (2003) 637–640.
- [8] E. Burstein, *Phys. Rev.* 104 (1956) 1508.